

EXPERIMENTAL EVALUATION OF DYNAMIC G_I FOR
THE INTERLAMINAR CRACK PROPAGATION
IN FIBRE COMPOSITES

by

SAVANUR RAJENDRAKUMAR A.

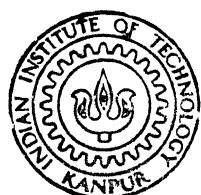
ME

1989

M.
RAT
S.

RAJ

Exp



DEPARTMENT OF MECHANICAL ENGINEERING

INDIAN INSTITUTE OF TECHNOLOGY, KANPUR

JANUARY, 1989

**EXPERIMENTAL EVALUATION OF DYNAMIC G_I
FOR THE INTERLAMINAR CRACK
PROPAGATION IN
FIBRE COMPOSITES**

**A Thesis Submitted
in Partial Fulfilment of the requirements
for the Degree of**

MASTER OF TECHNOLOGY

**by
SAVANUR RAJENDRAKUMAR A.**

**to the
DEPARTMENT OF MECHANICAL ENGINEERING
INDIAN INSTITUTE OF TECHNOLOGY, KANPUR**

JANUARY, 1989.

20 APR 1989

CENTRAL LIBRARY

LIBRARY KANPUR

Acc. No. A10.4240

ME - 1989 - M - ~~BAV~~ - EXP

**DEDICATED
TO MY
PARENTS**

21/1/89
D
2

CERTIFICATE

This is to certify that the thesis entitled "Experimenatal Evaluation of Dynamic G_I For The Interlaminar Crack Propagation In Fibre Composites" by Savanur Rajendrakumar A. is a record of work carried out under my supervision and has not been submitted elsewhere for a degree.

Prashant Kumar

Dr. Prashant Kumar
(Professor)
Dept. of Mechanical Engineering
Indian Institute of Technology
Kanpur - 208 016, India

2nd
January, 1989

ACKNOWLEDGEMENT

I express my deep sense of gratitude and appreciation to Professor Prashant Kumar, for his valuable guidance throughout the present work. His generous attitude has been a constant source of inspiration and encouragement.

I am thankful to Dr. Badri Rai, Dr. Shrivastava, Mr. Sharad C. Gupta, Mr. Madhusudan, Mr. Sanjay Verma for the help rendered in the experimental investigation.

Thanks to Mr. D.K. Sarkar and Mr. Rakesh Balmiki for their photographic work. I am also thankful to Mr. Swaran Singh and Mr. Jagir Singh for their co-operation needed in the experimental work.

Thanks to Mr. P.N. Panday, Mr. B.D. Panday for the help rendered in making the fine experimental set-up.

I am also thankful to Mr. Sharad C. Gupta for excellent typing of the manuscript.

- Savanur Rajendrakumar A.

CONTENTS

	Page
CHAPTER 1 INTRODUCTION	1
1.1 Fibre Reinforced Laminate	1
1.2 Mechanisms of Failure	2
1.3 Delamination a Major Failure Mode	2
1.4 Energy Release Rate G_I	3
1.5 Determination of Energy Release Rate G	5
1.6 Outline of the Present Work	6
CHAPTER 2 SPECIMEN MATERIAL	8
2.1 Reinforcement	8
2.2 Matrix Material	8
2.3 Hand Lay-up Technique	8
2.4 Bonding of Hinges	9
2.5 Crack Propagating Gauges	13
CHAPTER 3 EXPERIMENTAL TECHNIQUE	15
3.1 Expression for Dynamic G	15
3.2 Experimental Set-up	17
CHAPTER 4 RESULTS AND DISCUSSION	25
CHAPTER 5 CONCLUDING REMARKS	33
References	34

LIST OF FIGURES

Fig. No.	Title	Page
1.1	Modes of crack surface displacement.	4
2.1	Cast laminate with artificial crack through folded mylar sheet.	10
2.2	Double cantilever beam specimen.	11
2.3	Double cantilever beam specimen with hinges.	12
2.4	Specimen on location after impact.	14
3.1	Fixed load case of mode I.	16
3.2	Schematic diagram of the experimental set-up.	18
3.3	Overall view of the experimental set-up.	19
3.4	Weight and the platform.	21
3.5	LVDT with signal conditioner.	22
3.6	Circuit of the electronic box.	24
4.1	Oscilloscope traces of LVDT and Propagation gauges.	26
4.2	Dynamic G_{Ic} vs Crack velocity.	30
4.3	Relation between G_{Ic} and Crack velocity at the first crack propagation gauge.	31

ABSTRACT

An experimental set-up has been designed, constructed and perfected to measure dynamic G_{Ic} through constant load method. A DCB specimen with artificial crack was loaded by dropping a weight on a platform attached to the lower cantilever of the specimen while the upper cantilever is attached to the roof of a rigid frame. Crack opening displacement was measured through a LVDT and crack length of the advancing crack tip was monitored through four conducting gauges bonded in front of the crack tip at regular intervals. Glass fabric reinforced specimen exhibit sharp decrease of G_{Ic} with increasing crack velocity.

CHAPTER 1

INTRODUCTION

1.1 Fibre Reinforced Laminate

A composite material is created by assembly of two or more components - a selected reinforcing agent and a compatible matrix binder. This can achieve a combination of properties not achievable by any of the component materials acting alone.

Laminated fibre composites can now increasingly used in structural members of the aircrafts because they offer attractive properties such as high specific strength and stiffness, environmental stability etc.

There is growing demand for the composite materials which can replace metals in load bearing structures (for example in aircrafts structures). This has lead to the development of more sophisticated constituent materials and better designs. One of the common problems in using laminates is that they are susceptible to impact damage through delamination, that is, separation of laminae. In comparison to the conventionally used metals, the laminates are less tough and fracture cracks caused by an impact spreads to longer distances. This reduces the strength and stiffness and thus limits the life of a structure. Delamination in fibre composites has caused a concern amongst the designers to find the ways to delay or restrict the expansion of delamination.

For durability and damage tolerance considerations, delamination resistance has become the key issue when composite materials are used in structural applications [1].

1.2 Mechanisms of Failure

A great variety of deformation modes can lead to failure of the composite. The operative failure mode depends on the loading conditions and the microstructures of the composite, fibre diameter, volume fraction of fibres, fibre distribution etc. The material failure may be observed in many modes such as (i) breaking of the fibre, (ii) microcracking of the matrix, (iii) separation of fibres from the matrix (debonding) and (iv) delamination. The modes may act separately or jointly [2].

1.3 Delamination - A Major Failure Mode

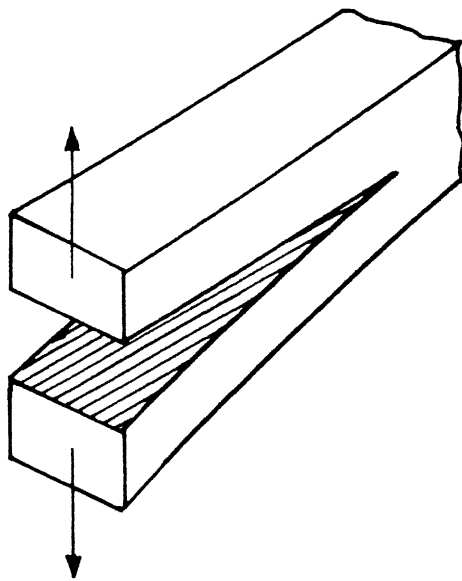
Due to the absence of through the thickness reinforcement, the laminate is prone to interlaminar failure or delamination. Delamination takes the form of separation of plies under mechanical, thermal or environmental loading. Potential sites for initiating an interlaminar crack may include geometric discontinuities, processing and machining defects and manufacturing flaws. The delamination also occurs due to impact on a laminate. This problem is unique to composites and is not observed in metals and polymers in general. Since the material properties are discontinuous in the thickness direction due to the laminated structure and since the interlaminar strength is generally very low in the interlaminar region, defects such as microcracks, voids, inclusions, broken plies etc. tend to grow in

an interlaminar mode. Also in the case of through the thickness impact, delamination can be a major failure mode.

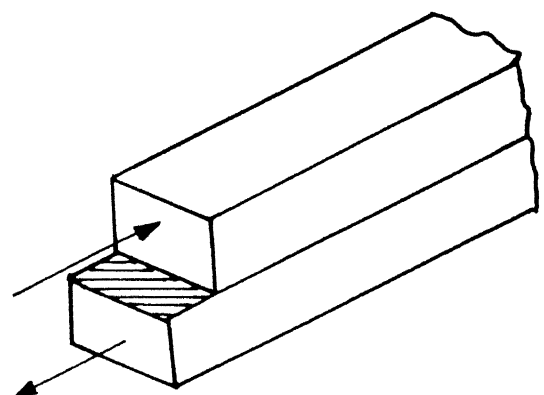
The interlaminar failure may occur through all the three well known modes (Fig. 1.1). In mode I failure is produced by a tensile stress applied at right angle to the laminate plane, resulting in opening up of the laminate. In mode II failure is caused by an in-plane shear stress (forwarded shear mode). In the mode III failure is in antiplane shear stress (parallel to shear mode). Generally, a failure is caused by the combination of all the three modes but delamination failure is known to be caused mainly by modes I and II.

1.4 Energy Release Rate G_I

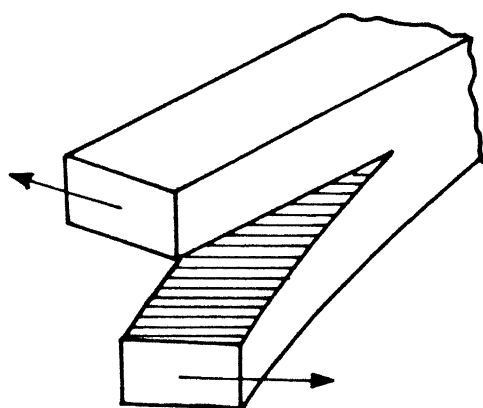
The equilibrium of an existing crack may be judged from the intensity of elastic stress around the crack tip (K) or by energy release rate G . Stress intensity factor K can be defined at the tip of delamination crack but the stress analysis in a composite material is difficult because of the local heterogeneity and anisotropy. Thus it has become common practice to characterize interlaminar fracture with the energy release rate G which is based on the energy consideration and is mathematically well defined as well as physically measurable by experiments. Further, in the application of the energy principle it is not necessary to specify the constitutive properties of the system. Also, the body may be isotropic or anisotropic, elastic or inelastic, linear or non linear.



(a) Mode I: symmetric loading
(opening mode)



(b) Mode II: skew symmetric
shear loading
(forward shear mode)



(c) Mode III : antiplane shear loading
(parallel shear mode)

Fig.1.1 Modes of crack surface displacement .

1.5 Determination Of Energy Release Rate G

Interlaminar fracture toughness is determined experimentally by suitable methods. Out of the three modes of interlaminar failure mentioned earlier, the mode I fracture toughness determination is well established under quasistatic conditions. G_{IIC} has been determined experimentally by a few investigators under quasistatic conditions but the experimental methods have not been standardized so far. For mode III fracture toughness methods are not developed because the need has not been felt. For evaluating G_{Ic} in composite materials, the double cantilever beam (DCB) type configuration is commonly used [3,4].

Keary et. al. [5] have used double cantilever beam specimen to measure interlaminar fracture toughness in mode I. They analysed the data through several different schemes and compared them with one another. For characterizing the behaviour of the delamination and fracture analysis for separation of modes, Wilkins et. al. [6] have found critical strain energy release rate for mode I and mode II delamination. They have used DCB specimen for mode I fracture study and cracked lap shear (CLS) specimen for mode II. Han and Koutsky [7] have found interlaminar fracture energy of glass fibre reinforce polyester composite. Devite, Schapery and Bradley [8] developed a non linear theory for energy release rate using DCB.

Guedra et. al. [9] have made a comparative study of various test methods for fracture toughness in mode I using DCB specimens. In order to study the various steps in the

delamination failure in mode I Charenteray and Benzeggagh [10] have further improved the accuracy of experimental techniques by monitoring crack propagation through acoustic emission. DCB specimen was also used in the investigation of loading rate effect. on the interlaminar fracture toughness by Mall, Law and Katouzian [11] and Smily and Pipes [12]. Recently, Narayan used DCB specimen made of glass fibre reinforced composites (GFRC) to evaluate G_{Ic} and ENF specimen of GFRC to get G_{IIc} experimentally [13].

For mode II interlaminar fracture, Carlsson et. al. [14] have used end notched flexure (ENF) specimen for finding mode II fracture toughness under quasistatic loading. They also analysed the effect of shear deformation and the influence of friction between the crack surface in the fracture toughness evaluation. The ENF specimen have also been used by Morom et. al. [15] to determine mode II interlaminar fracture toughness for various types of fracture toughness.

How G_{Ic} of interlaminar crack propagation varies with crack velocity is still an important problem not answered so far. The results are expected to provide deeper insight in explaining the damage caused by an impact of a foreign body on a laminate [16].

1.6 Outline Of The Present Work

In the present work specimens were made from fabric reinforcement laminate with artificial cracks in the mid-plane to find dynamic G_I . An experimental set-up has been designed and fabricated in which a double cantilever beam specimen was used.

The set-up was designed to operate on load controlled mode generated by dropping a weight. Crack length of the fast moving front is measured through breaking of conducting gauges bonded at the known intervals on the side face of specimen. COD is measured through a LVDT.

In chapter 2 the details of the specimen material are presented. In chapter 3 the details of the experimental set-up are described. The results of the work and discussion are given in chapter 4. Chapter 5 conclude the present work with the scope for future work.

CHAPTER 2

SPECIMEN MATERIAL

Glass fabric reinforced laminates were fabricated in our laboratory through the hand lay up technique for determining dynamic release rate in mode I. A crack was introduced in the composite laminate during the hand lay-up casting.

2.1 Reinforcement

Sixteen layers of fine woven glass fabric (purchased from FGP, Bombay) of 36x32 count/inch and 185 g/m^2 area density were used.

2.2 Matrix Material

Epoxy LY 556 with resin hardener HY 951 from CIBA, Bombay were used as matrix material.

2.3 Hand Lay-up Technique

Sixteen layers of glass fabric were cut to $380 \times 200 \text{ mm}$ sizes to make a laminate of about 3 mm thickness. Two thick steel plates (25 mm) each with one face flat and polished make the die of the casting. Glass fabric sheets are placed inside the die one after another. After a sheet is placed it is wetted with epoxy with the help of a brush and a specially designed metal roller.

In order to introduce the crack, a thin mylar sheet (0.025 mm thick) is folded and placed after the eight layers have been

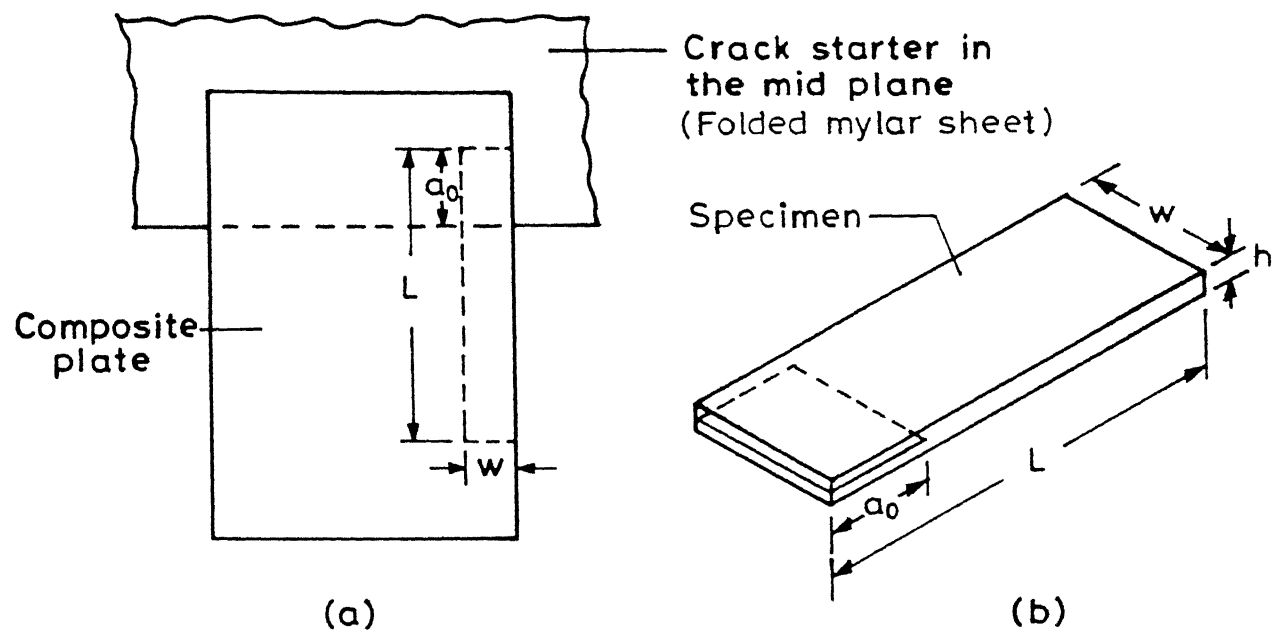
laid in the die. The mylar sheet was used in folded form to ensure no bonding between the cracked faces. The folded edge of the mylar sheet was placed parallel to one of the edges of the laminate about 110 mm inside as shown in Fig. 2.1. The last eight glass fabric sheets were placed one by one with proper wetting. The die was closed and the two faces were tightened by bolts. The die was heated to about 55° C through electric heating elements and a dimmerstat. The curing time was 24 hours. Fibre volume fraction of the resulting laminates was 40%.

The laminate is cut to obtain 5 specimen of sizes 200x30x3 mm as shown in Figs. 2.2 and 2.3. A diamond cutter was used for the purpose. The side faces were smoothened by sand papers of different grades.

2.4 Bonding of Hinges

For applying tensile load in opening mode, two metallic hinges (load tabs) were glued on both sides of the specimen on the crack side as shown in Fig. 2.3. The bonding surface of the hinges were roughened by punch and saw cuts (in ± 45 directions). The surfaces were first cleaned by soap and afterwards soaked, in acetone. Similarly, portions of specimen surfaces about to come in contact with hinge surfaces was rubbed with coarse sand paper in ± 45 directions. Also saw cuts were made in the same directions. The surfaces were washed with soap and then with acetone.

The hinges were attached to the specimen through Araldite adhesive available in the tube form. The hinges were aligned



$$L = 190 \text{ mm}$$

$$a_0 = 65 \text{ mm}$$

$$w = 30 \text{ mm}$$

$$h \approx 3 \text{ mm}$$

Fig. 2.1 Cast laminate with artificial crack through folded mylar sheet.

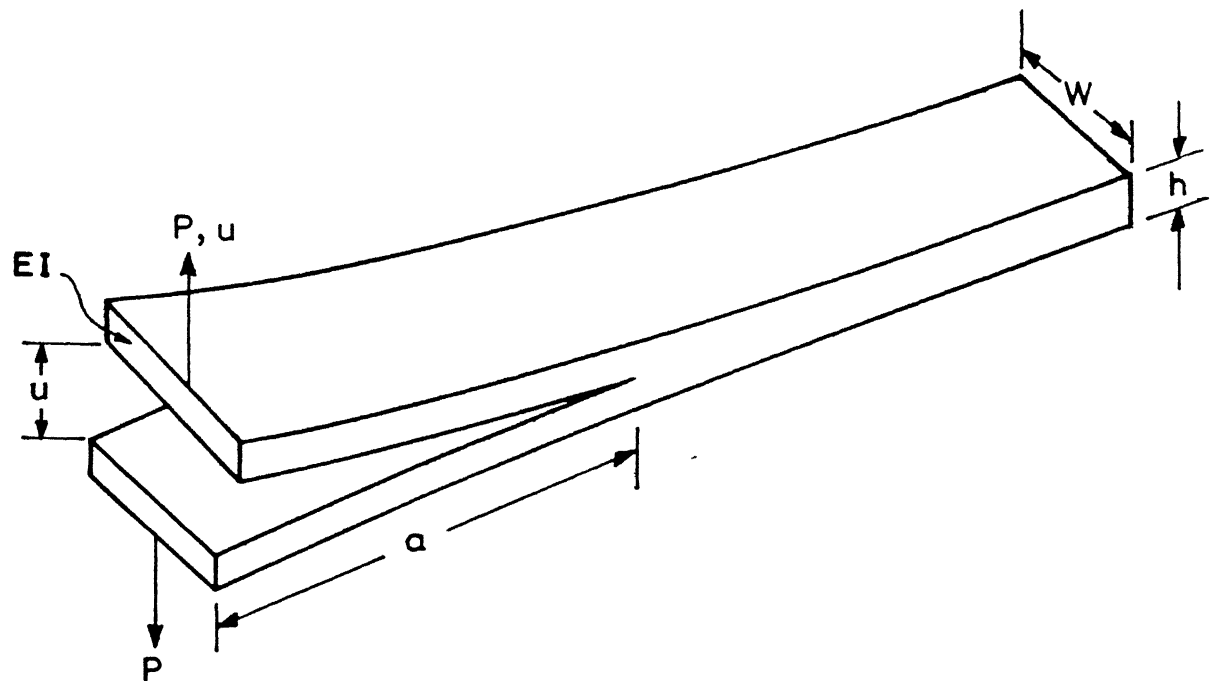


Fig. 2.2 Double cantilever beam specimen.

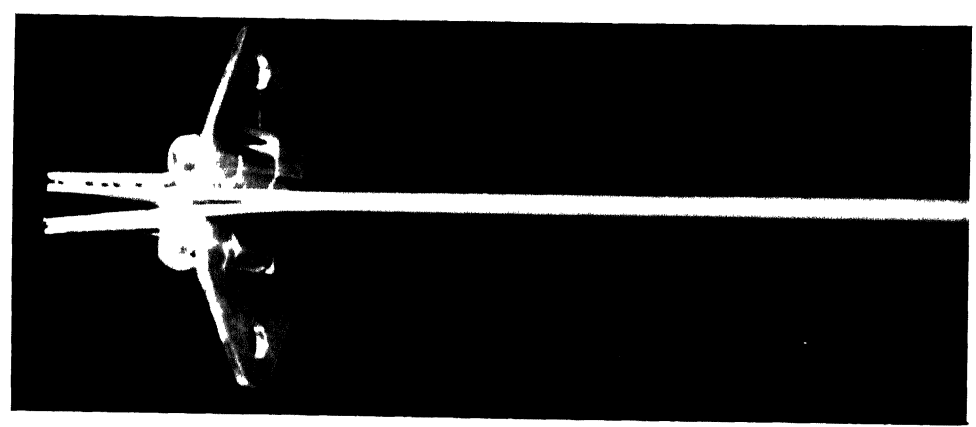


Fig. 2.3 Double cantilever beam specimen with hinges.

properly by using a specially designed mounting jig which applies pressure through C-clamps. The curing takes about 24 hours.

2.5 Crack Propagating Gauges

In order to monitor the crack length during dynamic propagation of interlaminar crack, four gauges were used on one side of the specimen at the interval of 10 mm apart. Each gauge is a conducting sheet of aluminum of Ø.025 mm thickness. A thin strip of about 1 mm width is bonded to the specimen. Prior to the bonding, the surface was degreased with acetone for good bonding. Fast curing Fevicol 702 CYN was used for bonding which needs a constant hand pressure for about 10 seconds. Care was taken to have uniform bonding of the strip with the specimen. An advancing crack front tears through the gauge breaking the electrical circuit between the two ends of the gauge. The information is carried to an oscilloscope. Fig. 2.4 shows all the four gauges broken during the dynamic loading of the specimen.

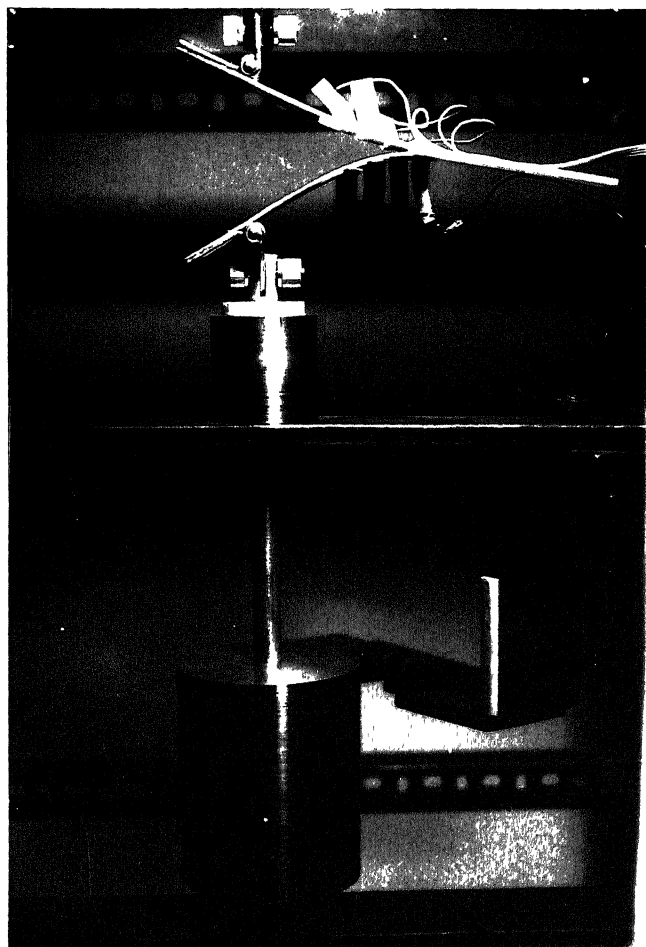


Fig. 2.4 Specimen on location after impact.

CHAPTER 3

EXPERIMENTAL TECHNIQUE

A method has been developed to determine G_{Ic} at high speed of crack propagation in fibre composites using DCB specimens.

3.1 Expression for Dynamic G_I

A potential energy ϕ is defined for a specimen with a crack as

$$\phi = U - W_{ext} \quad (3.1)$$

where U is the elastic strain energy stored in the body and W_{ext} is the work supplied by the external force. If G_{Ic} is the work required to create a unit crack area, the criterion for crack growth can be written as

$$\delta\phi \geq G_{Ic} \delta A$$

where δA is the increase in crack area. For critical conditions the equality sign and for unstable crack growth inequality sign holds good.

The strain energy release rate, G_I is defined as

$$G_I = -(\delta\phi/\delta A) \quad (3.2)$$

In terms of G_I , the fracture criterion may be formulated as

$$G_I \geq G_{Ic}$$

The configuration of loading a specimen in mode I is shown in Fig. 3.1. The specimen was loaded by dropping a weight.

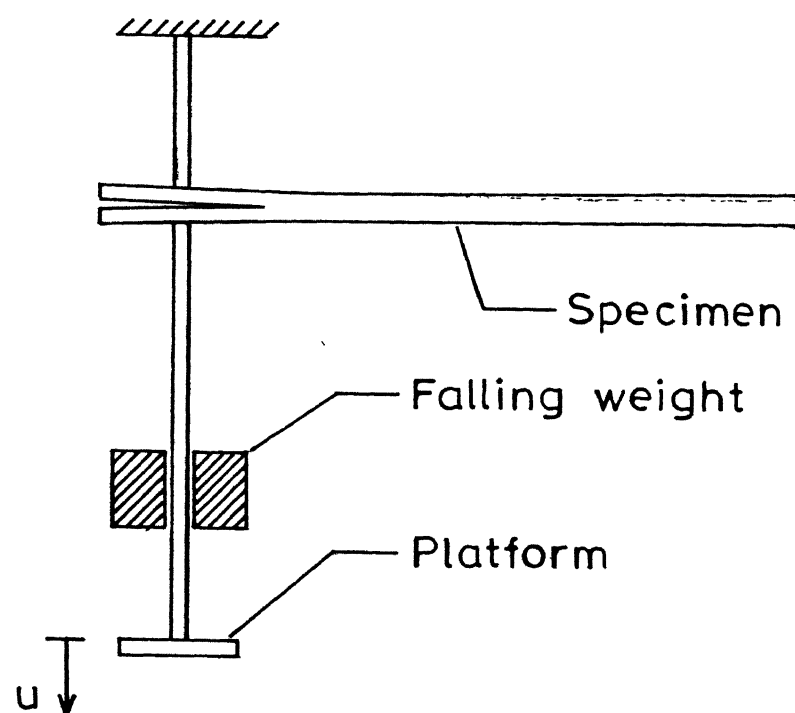


Fig. 3.1 Fixed load case of Mode I

The displacement of the platform u provides the crack opening displacement (COD). If v_0 is the velocity of the dropping weight just before it touches the platform Eq. 3.1 changes to

$$\phi = U - [Pu + \frac{1}{2}m_0v_0^2 - \frac{1}{2}mv^2] \quad (3.3)$$

where m_0 is the mass of the weight, m is the combined mass of the weight and the platforms, P is the force applied by the weight and v is the velocity of the platform.

Substituting strain energy density $\frac{1}{2}Pu$ in Eq. 3.3, one obtains,

$$\begin{aligned}\phi &= \frac{1}{2}Pu - [Pu + \frac{1}{2}m_0v_0^2 - \frac{1}{2}mv^2] \\ &= -\frac{1}{2}Pu - \frac{1}{2}m_0v_0^2 + \frac{1}{2}mv^2\end{aligned}$$

G_I is obtained by differentiating ϕ and substituting in Eq. 3.2 as

$$G_I = (P/2w) (\delta u / \delta a) - (m/2w) (\delta v^2 / \delta a) \quad (3.4)$$

3.2 Experimental Set-up

Upper cantilever of a DCB specimen is suspended from the top of the main frame made rigidly from slotted angles as shown in Fig. 3.2 and 3.3. The specimen remains horizontal. To guard against the development of unwanted loads, the top support has two horizontal hinges with their axes mutually normal to each other. The load is applied to the bottom cantilever through a platform. Again the platform is attached to the specimen through two mutually orthogonal horizontal hinges to avoid generation of

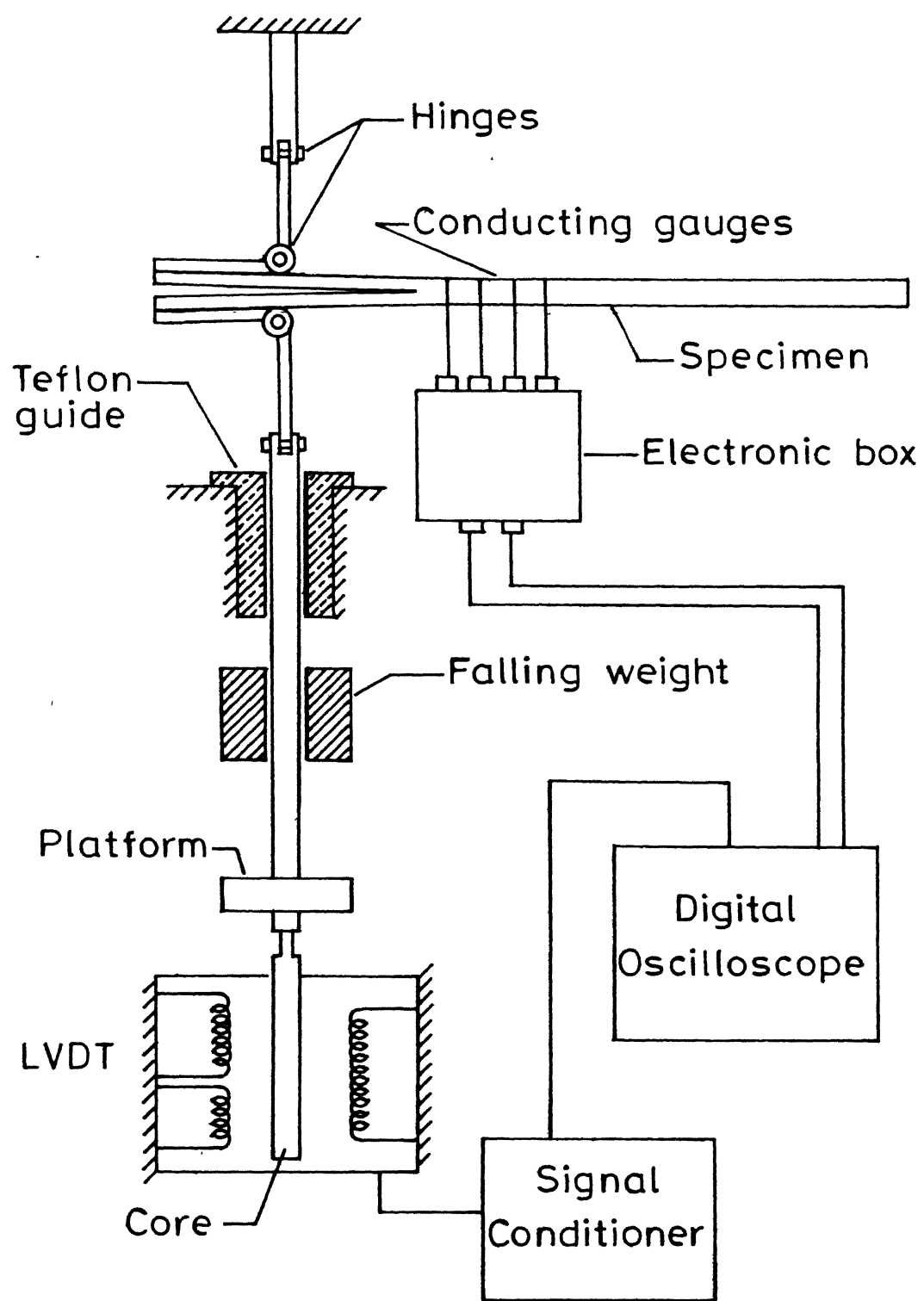


Fig. 3.2 Schematic diagram of the experimental set-up .

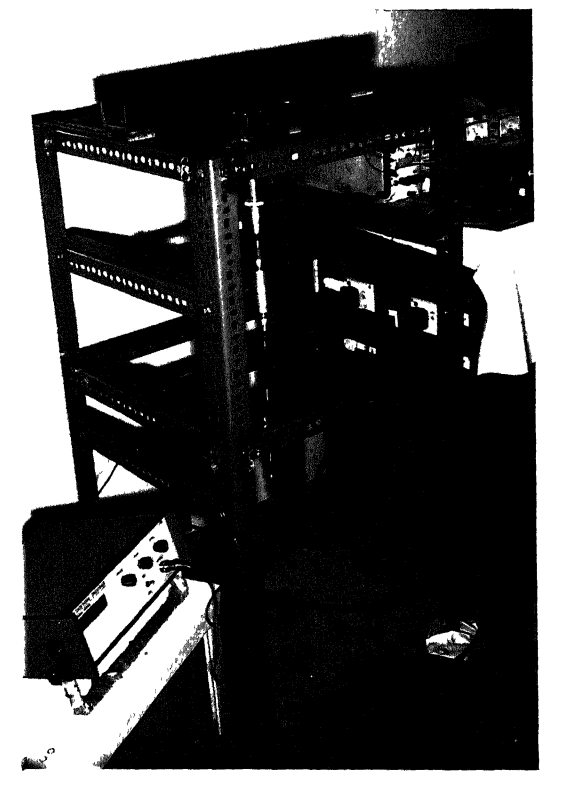


Fig. 3.3 Overall view of the experiment setup.

bending moments and shear loads.

Dead weights (2 kg., 3 kg. and 4 kg.) were dropped one at a time from a known height on the plateform along its guide rod (Fig. 3.4). Care was taken to see that the weights slides along the rod smoothly without much clearance. The weight is cylindrical and is made of mild steel. Its faces were made slightly convex so that when the weight impact the base of the platform, most of the energy is imparted close to the axis of the platform.

To measure the displacement of the platform, which is same as COD, the core of a linear variable differential transformer (LVDT) is attached to the bottom of the platform as shown in Fig. 3.2 and 3.5. The outer casing of the LVDT is fixed rigidly to the main frame. The LVDT was purchased from New Engineering Enterprises Roorkee (Model No. DL 25). Its core was built from a thin wall tube to have low intertia. Its total displacement range is 60 mm with a guaranteed linear range of $0 - 50$ mm. The LVDT is used with a signal conditioner for an analog output of $\pm 2V$ to an oscilloscope. The LVDT is very sensitive and can measure upto 1 μm .

During the dynamic crack propagation, the length of the crack as function of time is monitored through four conducting gauges shown in Fig. 3.2. As soon as the first gauge breaks, the signal is sent to a digital oscilloscope through an electronic box. Similar signals are sensed by the oscilloscope successively when the second, third and fourth gauges are broken.

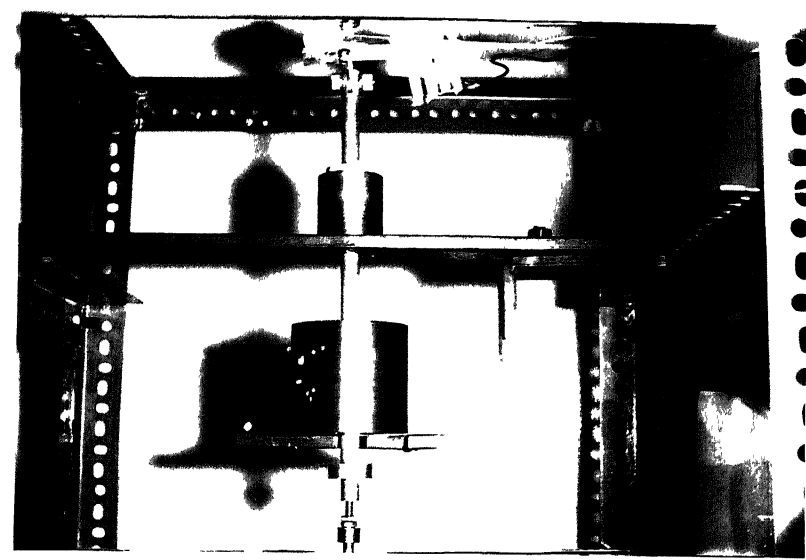


Fig. 3.4 Weight and the platform.

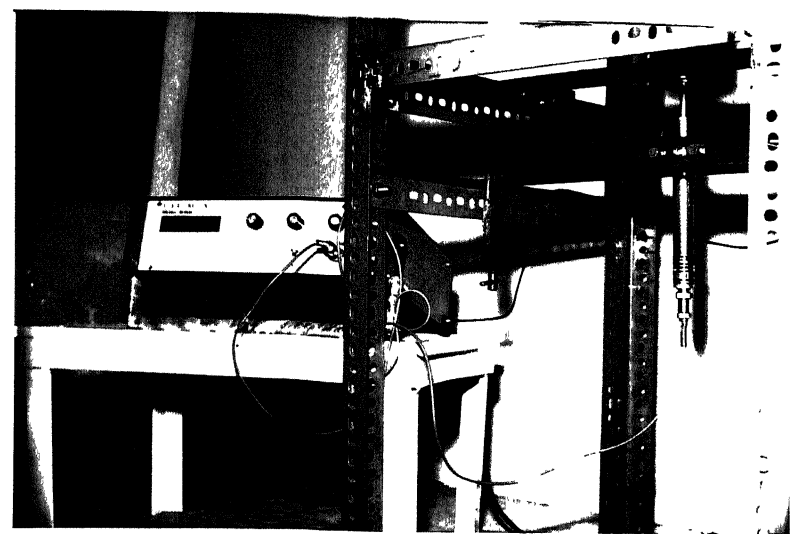


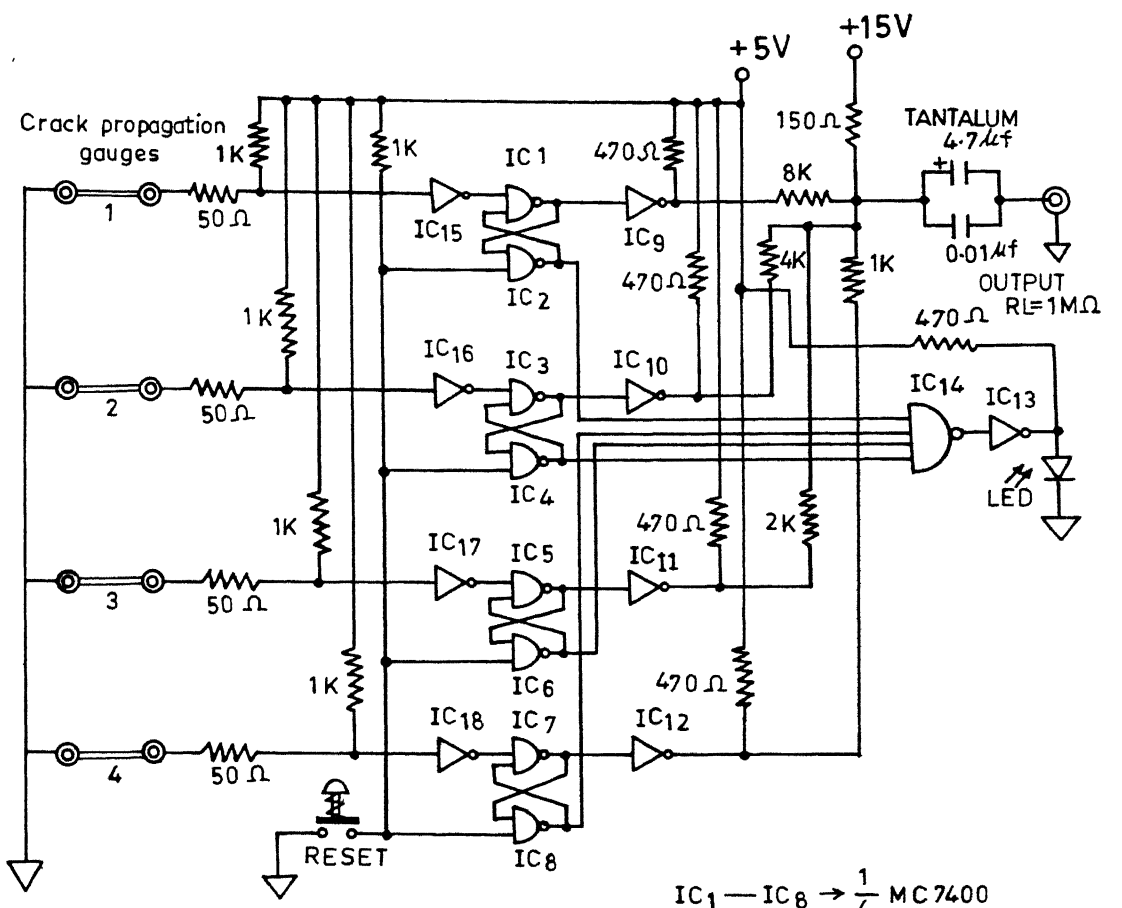
Fig. 3.5 LVDT with signal conditioner.

The electronic box is designed to convert four inputs from the gauges into one. When the first signal arrives at the electronics box, the voltage at the output drops from an initially high value of 2 volts by about 0.4 volts. The breakage of the second gauge causes an additional drop of about 0.3 volts. Thus, the voltage output from the electronics box gives a descending steps like input to the oscilloscope.

The electronic box was designed to have a very fast response time (less than 1 μ s) through the use of integrated circuit chips. The details of the circuit are shown in Fig. 3.6.

Digital oscilloscope (Nicolate 2090 - IIIA) was found very suitable to record both the signals - one from the LVDT and another from the electronic box. They were recorded on the dual beam mode. Triggering of the oscilloscope was conducted through the breakage of the first conducting gauge by the advancing crack front. This causes the drop in voltage output of the electronic box which in turns triggers the oscilloscope through internal triggering. Due to inbuilt feature of the oscilloscope with memory, the LVDT response was measured even before the oscilloscope was triggered.

The platform along with a weight is stopped after it moves beyond the expected crack opening displacement to protect LVDT and the teflon sleeve from damage. A 6 mm thick rubber sheet is placed between the platform and the stop.



$IC_1 - IC_8 \rightarrow \frac{1}{4}$ MC7400
 $IC_9 - IC_{13} \rightarrow \frac{1}{6}$ MC7405
 $IC_{14} \rightarrow \frac{1}{2}$ MC7420
 $IC_{15} - IC_{18} \rightarrow \frac{1}{6}$ MC7404

Fig.3.6 Circuit of the electronic box .

CHAPTER 4

RESULTS AND DISCUSSION

The set-up has been designed to record COD and crack length of a DCB specimen as a function of time to evaluate dynamic G_{Ic} of glass fabric reinforced laminates. The COD was measured by a LVDT while the crack length was monitored by four conducting gauges placed at equal intervals. Both the records were made on a dual beam digital oscilloscope. A typical oscilloscope response is shown in Fig. 4.1 which has been obtained by transferring it from the memory of the storage oscilloscope to a X-Y recorder. Output of the LVDT is linear. As expected, the response of the crack propagation gauges was in the form of descending steps; each step indicates the breaking of the gauge by the advancing crack front. The large drop of voltage at the first gauge triggers the oscilloscope through internal triggering.

The velocity of the crack tip can be controlled through two parameters, (i) weight and (ii) the height up to which the weight is raised. The height controls the kinetic energy of the weight just prior to the impact.

Experiments have been conducted with two weights, 3 kg and 4 kg. In each case, the height of the dropping weight was varied between 17 and 45 mm. Table 4.1 provides the details of all the six experiments.

The values of crack velocity \dot{a} was obtained from the

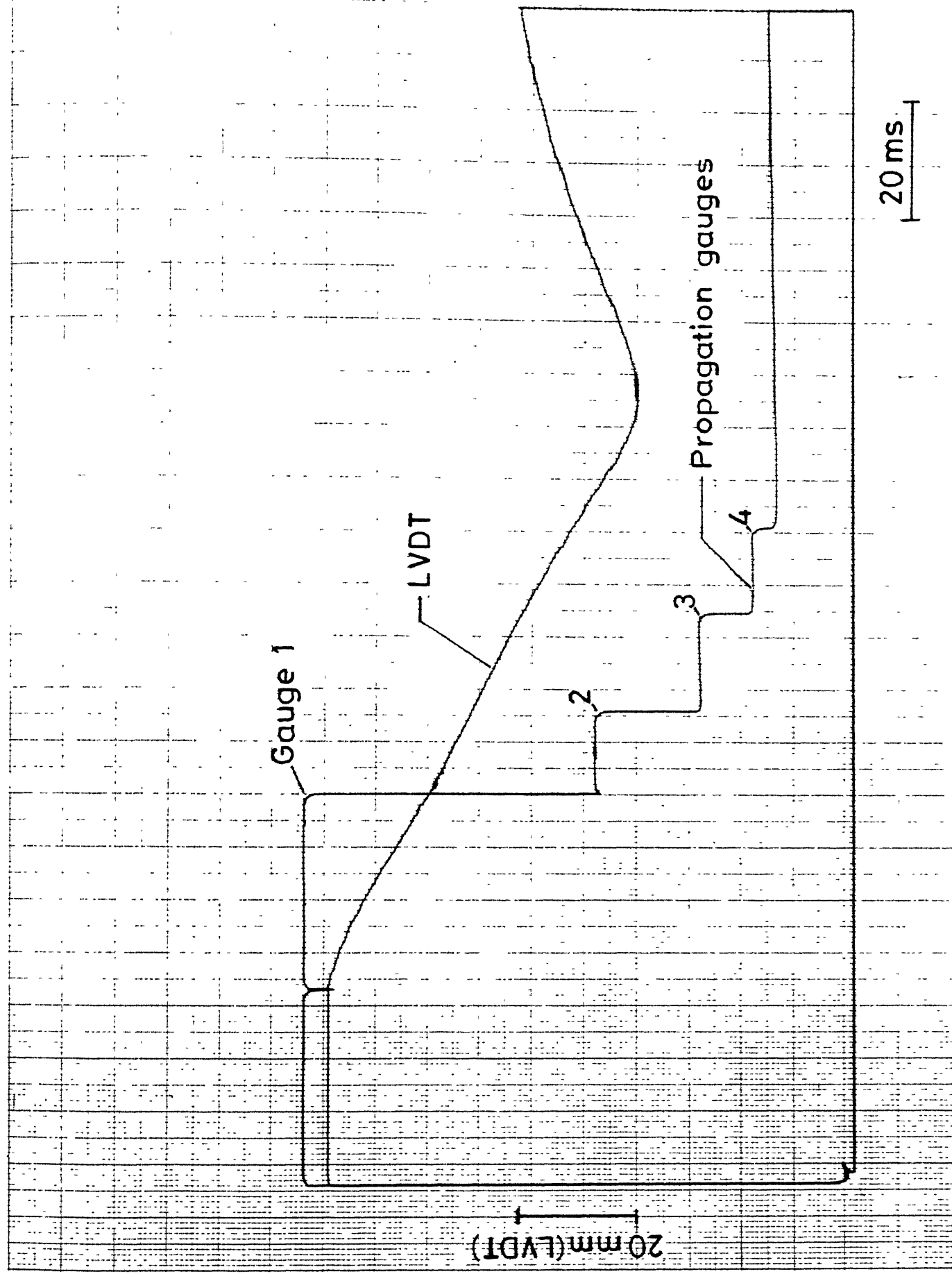


Fig. 4.1 Oscilloscope traces of LVDT and propagation gauges

TABLE 4.1

S.No.	Exp.No.	Weight kg	Height mm	a m/sec				δ_{IC} J/m^2			
				Gauge 1	Gauge 2	Gauge 3	Gauge 4	Gauge 1	Gauge 2	Gauge 3	Gauge 4
1	808	3	17	0.95	0.90	0.52	0.27	248	476	693	932
2	810	3	45	0.85	1.50	1.88	2.24	1569	1138	747	335
3	811	3	40	0.42	1.28	1.56	2.01	1504	1003	525	23
4	812	4	20	0.51	0.51	0.50	0.50	991	843	680	510
5	813	4	25	0.77	0.68	0.60	0.48	446	552	649	755
6	815	4	32	1.76	1.46	1.00	0.33	187	471	768	1028

measured time corresponding to the breakage of the conducting gauges placed at premeasured crack lengths. A quadratic curve was fitted using the least square method to obtain a smooth curve for crack length as a function of time. The relation was differentiated to determine crack velocities.

For calculating dynamic G_{Ic} , Eq. 3.4 was used. The first term ($\delta u / \delta a$) was calculated from the experimentally measured crack opening displacements u 's at four crack lengths. A smooth curve u vs a relation was obtained by fitting a quadratic curve through the least square method. Then the differentiation of u with respect to a provides the first term. For evaluating the second term, a similar procedure was adopted. A quadratic curve was fitted to find smooth u vs t relation which in turn, provides velocity v after differentiation. The same procedure was carried out one more time to evaluate smooth v^2 vs a curve and then differentiated to obtain the second term.

It is to be noted that the crack velocity \dot{a} changes with the crack length. In Expts. 810 and 811, \dot{a} increases with the increasing crack length while in Expts. 808, 813 and 815 \dot{a} decreases with the crack length. In Expt. 812 crack velocity does not change. This can be explained through the two parameters of load application, value of the dropping weight W and height H from which the weight is dropped. When the dropping height is small, the crack velocity decreases with the crack length. For high value of H , the weight acquires high enough kinetic energy at the time of impact to make the crack move faster with the crack length. Expt. 812 is the case of moderate

height for which the crack velocity does not change. Even in Expt. 813 H is moderate and the crack velocity decreases marginally with crack length.

From the data analysis point of view, it is desirable to minimize the second term of Eq. 3.4 because it involves differentiation of experimental data twice. However, it is difficult to make the crack move at high speeds without the help of kinetic energy of the falling weight.

The results of table I are shown in Fig. 4.2. In all the experiments the dynamic G_{Ic} decreases with increasing crack velocity except for the case of Expt. 812 in which the crack velocity does not change. A straight line is fitted to each case as shown in the Fig. 4.2. The average value of the rate of change of dynamic G_{Ic} with respect to crack velocity is -920 Js/m^3 .

The quasistatic G_{Ic} obtained by Narayanan [13] through the displacement controlled method is also shown in Fig. 4.2. The specimen materials were identical to the materials used in this study as the same casting procedure and raw materials were used. However, dynamic G_{Ic} at low crack velocities are higher than quasistatic G_{Ic} . The behaviour is not understood.

G_{Ic} value at the first conducting gauge which is close (within 12 mm from the crack tip of unadvanced crack) to the crack tip may provide a better representation of dynamic toughness of the material. Fig. 4.3 shows the relation between dynamic G_{Ic} and the crack velocity at the first conducting gauge.

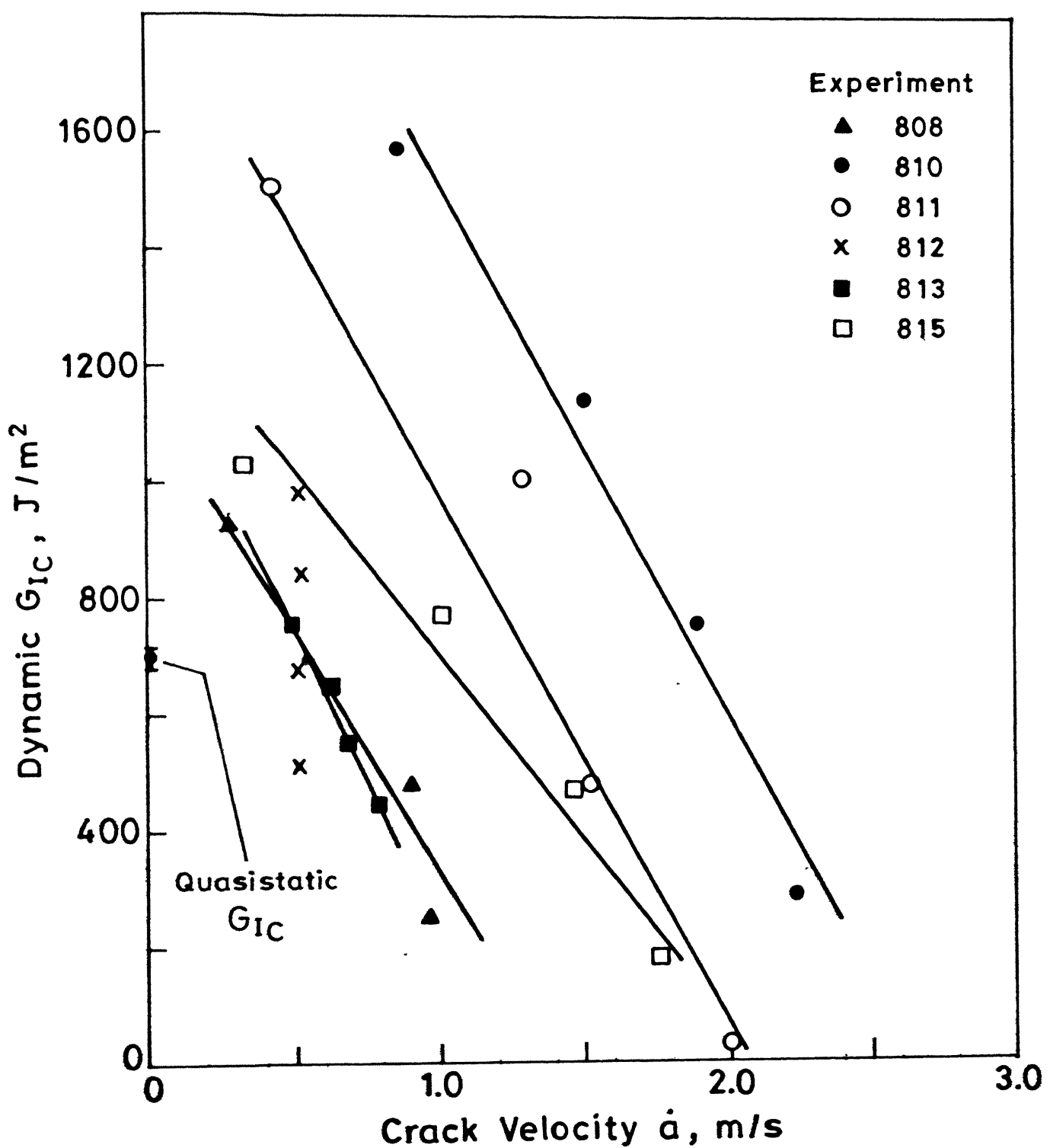


Fig. 4.2 G_{IC} vs. crack velocity .

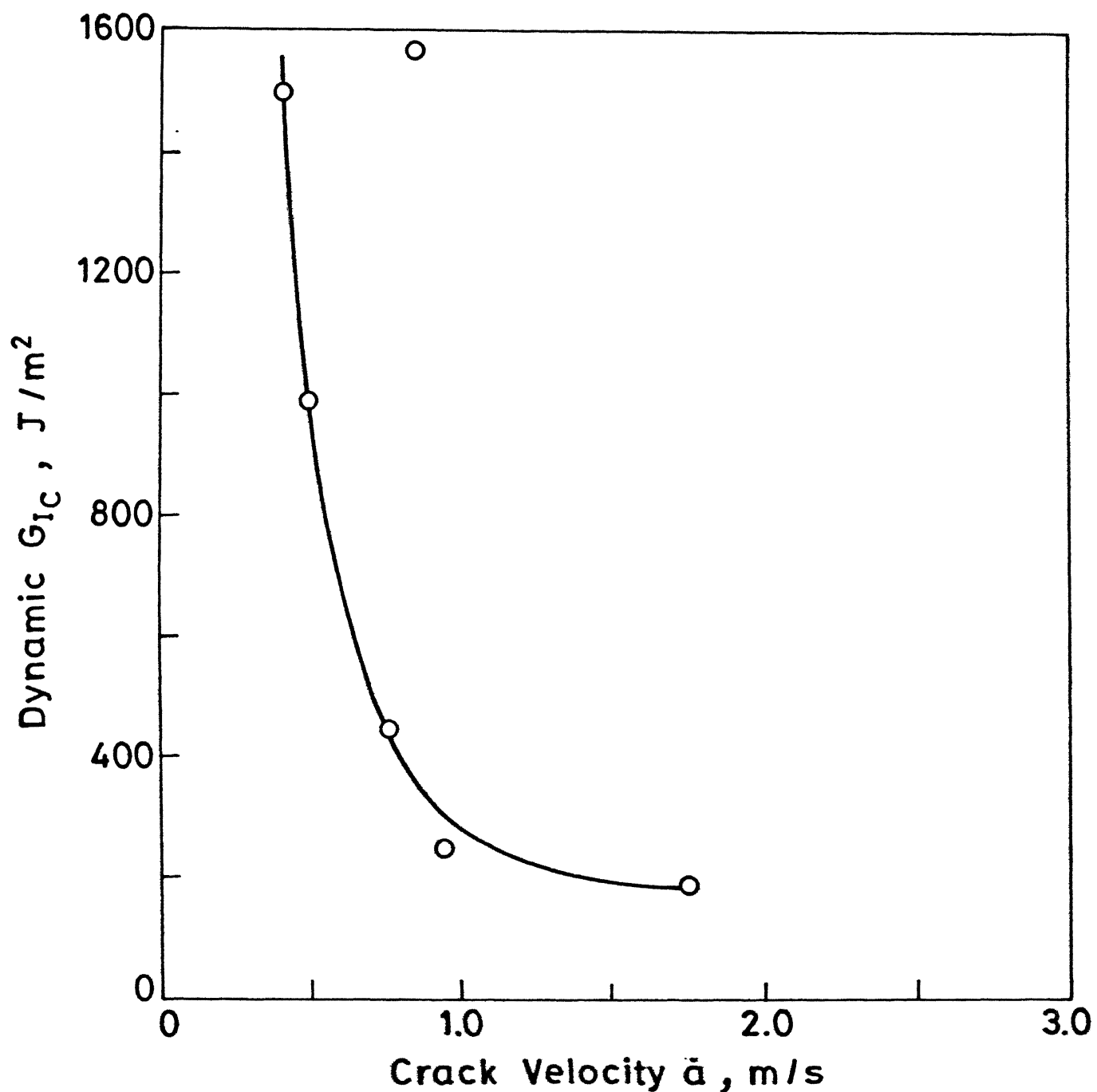


Fig. 4.3 Relation between G_{IC} and crack velocity at the first crack propagation gauge.

Dynamic G_{Ic} decreases sharply from 1500 to 190 J/m^2 as the crack velocity increases from 0.4 to 1.8 m/s.

CHAPTER 5

CONCLUDING REMARKS

An experimental set-up has been designed, constructed and perfected to measure dynamic G_{Ic} through constant load method. A DCB specimen with artificial crack was loaded by dropping a weight. Crack opening displacement was measured through a LVDT and crack length of the advancing crack tip was monitored through four conducting gauges bonded in front of the crack tip at regular intervals. Glass fabric reinforced specimen exhibit sharp decrease of G_{Ic} with increasing crack velocity.

It has been shown that the technique of finding dynamic G_{Ic} works. However, it needs to be modified. In the present setup, even the highest crack velocity (2.24 m/s) is very low in comparison to the velocities of delamination crack front measured through high speed photography when the laminate is impacted ballistically by a forgien body [16]. The cracks were observed to move upto 300 m/s. In the present set-up, the platform should be modified to accommodate much larger weights than 4 Kg together with the capability of dropping the weight through much larger heights.

The data analysis also needs modification. Both cantilevers of a DCB specimen deflect by large distance and rotate by fairly large angles. Thus, geometrical nonlinearity requires more elaborate data analysis.

REFERENCES

1. John E. Masters, "Correlation of Impact and Delamination Resistance in Interleafed Laminates", VI ICCM, 3 (1987), 96-107.
2. Agarwal, B.D., and L.J. Broutman. "Analysis and Performance of Fibre Composites", John Wiley and Sons, New York, (1980).
3. Bascom, W.D., Bitner, J.L., Moulter, R.A. and Siebert, A.R., "The Interlaminar Fracture of Organic Matrix Woven Reinforcement Composites", Composite, January 1980.
4. Sidney J.E. and Bradshaw. F.J., 'Some investigations on carbon-fibre reinforced plastics under impact loading, and measurement of fracture energies.', Proceeding of the international conference organised by the Plastic Institute of London on feb. 2, 3, 4, 1971.
5. Paul E. Keary and Lary B. Ilicewicz, Casey Shear and Jess Trostle, 'Mode I interlaminar fracture toughness of composites using slender double cantilever beam specimen.', J. of composite materials., 19 (Mar. 85), 154-177.
6. Wilkins, D.J., J.R. Eisenmann, R.A. Camin, W.S. Margolis and R.A. Benson. "Characterising Delamination Growth in Graphite Epoxy", Damage in Composite Materials, ASTM STP 775, 1982, 168-183.
7. Han, K.S. and J. Koutsky. "The Interlaminar fracture Energy of Glass Fiber Reinforced Polyester Composites", J. Composite Materials, 15 (1981), 371-388.
8. Devitt, D.F., R.A. Schapery and W.L. Bradley. "A Method For Determining the Mode I Delamination Fracture Toughness of Elastic and Viscoelastic Composite Materials", J. Composite Materials, 14 (1980), 270-285.
9. Guedra, D., D. Lang, J. Rouchon, C. Marais and P. Sigety, "Fracture Toughness in Mode I : A Comparison Exercise of Various Test methods", VI ICCM, 3 (1987), 347-357.
10. De Charentenay, F.X. and M. Benzeggagh. "Fracture Mechanics of Mode I Delamination in Composite Materials", IV ICCM, (9180), 186-197.
11. S. Mall, G.E. Law and M. Katouzian, 'Loading rate effect on interlaminar fracture toughness in thermoplastic composite', J. of composite materials, 21 (1987), 569-579.
12. A.J. Smiley and R.B. Pipes. 'Rate effect on Mode I interlaminar fracture toughness in composite materials', J. of composite materials, 21 (1987), 670-687.

- 13 M.D.Narayan, 'Energy release rates in delamination crack propagation of glass fabric reinforced composites.', M.Tech.Thesis,1988,IITK.
14. Carlsson, L.A., Gillespie, J.W. Jr. and Pipes, R.B., "On The Design And Analysis Of The End Notched Flexure (ENF) Specimen For Mode II Testing", J. Composite Matreial, 20 (1980), 594-604.
15. Marom, G., I. Roman, H. Harel, M. Rosensaft, S. King and Moshonor. "The Characeterization of Mode I and Mode II Delamination Failures in Fabric-Reinforced Laminates", VI ICCM 3 (1987),265-273.
16. Takeda, N., R.L. Sierakowski and L.E. Malvern. "Delamination Crack Propagation in Ballistically Impacted Glass/Epoxy Composite Laminates", Experimental Mechanics, 22 (1982), 22-25.